An Enhanced Second Carrier Harmonic Cancellation Technique for Dual-Channel Enhanced Power Generation Centre Applications in More-Electric Aircraft

Cheng Wang, Tao Yang, *Senior Member, IEEE,* Ponggorn Kulsangcharoen, *Member, IEEE,* and Serhiy Bozhko, *Senior Member, IEEE*

***Abstract*— The more-electric aircraft concept has made the extraction of electrical power from both high-pressure shaft and low-pressure shaft of the aircraft engine essential for future aircraft. With each shaft driving one electrical generation channel, an advanced dual-channel enhanced power generation system can be formed. This paper aims to address the power quality issues of this dual-channel power generation system, specifically focuses on the reduction of harmonics on a common dc bus. A simplified model to estimate second carrier harmonic of dc current in two-level converters is developed and reveals the fact that while this second carrier harmonic component magnitude can be determined by modulation index and dc-link current, its phase angle is solely dependent on the angle of carrier signals. Based on the developed model and these key findings, a new harmonic cancellation method is proposed through active power sharing and phase angle shifting of the carrier signals within different power sources. The method has demonstrated high robustness and is effective under different fundamental frequencies and power sharing ratio. Both simulation and experimental results are presented in this paper to validate the proposed harmonic model and the enhanced cancellation method.**

***Index Terms*— More-electric aircraft, dual-channel, capacitors, second carrier harmonics, simplified model, cancellation method.**

I. Introduction

The more-electric aircraft (MEA) concept has been accepted as the general trend of future aircraft [1]-[3]. Functions such as environment control and flight actuation, which used to be driven by pneumatic and hydraulic power, are being replaced with electrically driving subsystems. The implementation of MEA concept will result in significant increase of electrical power demand on-board. Electrical power on aircraft is normally extracted from the high-speed shaft of an aircraft engine. The increased electrical loads onboard require more power to be extracted from the engine high-speed shaft which will create stability issues for the engine. To avoid this issue, power extracting from the low-pressure shaft (which operates with much wider speed range compared with high-pressure shaft) becomes inevitable. The recent advancement in power electronic, machine and control has enabled engineers to investigate the possibility of extracting electrical power from the engine low-pressure shaft[4]-[6]. In paper [6], authors proposed an advanced dual-channel electric power generation architecture as shown in Fig. 1. In the proposed system, two electrical generators are driven by two engine shafts, i.e. high pressure (HP) shaft and low pressure (LP) shaft respectively. These two generators supply one common DC bus through their own power electronic converters. The authors have concluded that this architecture enables dual-channel power generation and power transferring between two engine shafts. The enabled power transfer between two engine shafts will result in improved engine efficiency and stability, as well as compatible thrust with flight mission[6][7]. Then, the fuel consumption and maintenance fee can be reduced for the aircraft. Although with mentioned advantages, system optimization is still essential, especially to DC capacitors on the common DC bus, which is always bulky and expensive. For aircraft applications, the weight and volume of devices, the dc-bus capacitor in this case, are critical design factors which should be minimized during the design process. Minimizing harmonics of dc-bus currents

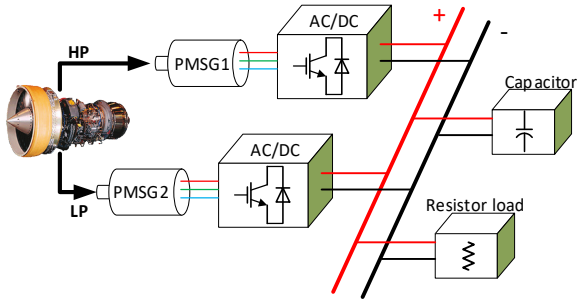

Fig. 1. Dual-channel enhanced power generation system.

This work was supported by the Clean Sky 2 Joint Undertaking under Grant 807081. (Corresponding author: Tao Yang.) The author Cheng Wang also thanks the stipend funding from China Scholarship Council (CSC).

C. Wang, T. Yang, S. Bozhko are with the Power Electronics, Machines and Control Group, The University of Nottingham, Nottingham NG7 2RD, U.K. (e-mail: cheng.wang@nottingham.ac.uk; tao.yang@nottingham.ac.uk; serhiy.bozhko@nottingham.ac.uk).

P. Kulsangcharoen is with Collins Aerospace, Shirley, Solihull, UK (e-mail: ponggorn.kulsangcharoen@utas.utc.com).

can potentially reduce the size of the capacitor required such that the DC-bus voltage meet the MIL-STD-704F standard. The suppression of harmonics at the DC bus will further improve power quality on the bus and minimize the size of the capacitor. Meanwhile, another benefit gained from suppressed dc-bus current harmonics is increasing capacitor lifetime, which is critical for electrical power system reliability. There are numerous methods proposed to minimize current ripples on capacitors[8][9]. However, the control bandwidth of those methods is mostly below the switching frequency. This means that current harmonics due to switching behaviour of converters are filtered out in the control loop and these algorithms are not able to mitigate such current harmonics flowing into to the DC-bus capacitor. This paper aims to fill this gap and propose a simple method which can suppress the switching harmonics of the current flowing into the capacitor.

In recent years, researchers have published several papers on reduction of switching harmonics for two-level converter dc-link capacitors. In [10], a mathematical model of DC-link currents is developed using a double Fourier solution. It gives researchers room to analyse and minimise the current harmonics for a single two-level AC/DC converter. In [11], low capacitor harmonics are achieved by implementing a high modulation index on DC-AC inverter using an additional DC-DC converter. The disadvantage with this method is that more switching devices are required and thus comes with extra cost. In [12], the capacitor current ripple is reduced by applying nonadjacent switching vectors. In [13], analytical expressions for a phase shift of the boost converter are derived which lead to a minimum capacitor current. However, all these papers focus on single converter operations with one AC source. They are not suitable for dual-channel generation systems with multiple generators and AC/DC converters.

For multi-source DC electrical power systems, the fundamental frequencies of generators are always assumed to be the same in most of the recent publications[14]-[17]. However, this normally is not the case for dual-channel power generation architecture of the type considered in this paper. In the proposed architecture, the electrical generators are supplied by generators driving by different shafts, thus with different fundamental frequencies. For multi-source systems with the same fundamental frequencies, the interleaving concept is one way to suppress harmonics on switching frequency[14][15]. However, for a system as shown in Fig. 1, different fundamental frequencies are applied to the converters. To the best of authors' knowledge, there is so far very limited publications addressing this issue and illustrating how to minimize the switching harmonics.

Although this paper focuses on the dc-bus supplied by two generators through power converters, the proposed method and analysing technique can be extended to back-to-back converters, which is commonly used in the motor drive systems. Indeed, a back-to-back converter can be regarded as a multi-source power system, where a rectifier and an inverter share one DC-bus capacitor and frequencies of input and output voltages are unequal. Shen investigated methods of eliminating the switching frequency components of the first order[18] and the second order[19] harmonics by synchronizing the carriers' phase based on band-pass filter and phase angle measurement. However, the performance highly relies on the quality of the band-pass filter, which limits the application of this method.

In this paper, an enhanced cancellation method for 2nd carrier harmonics on the capacitor is developed to suppress the current harmonics over dc-link capacitor. The proposed method does not require two generators sharing the same fundamental frequency. A simplified mathematic model of 2nd carrier harmonics on DC-bus is investigated and developed in section II, which helps simplify the calculation procedure. With the simplified model, a new method to minimize the 2nd carrier harmonic is proposed in section III. With the proposed model and method, significant harmonic minimization can be achieved under any fundamental frequency and power sharing ratio. Compared with the method proposed by Shen in [18] and [19], measurement of phase angle of harmonic on DC bus is not required, which makes this method easily applicable on low communication bandwidth system. Lastly, the proposed method has been validated by simulation and experiment with results given in Section IV.

II. 2ND CARRIER HARMONICS ANALYSIS OF SINGLE CONVERTER

In order to develop a mechanism to suppress harmonics at the dc bus, thorough knowhow of single two-level converter and how the current harmonics are generated is essential[20]. A two-level three-phase converter and asymmetrical regular sampling PWM are shown in Fig. 2a and b.

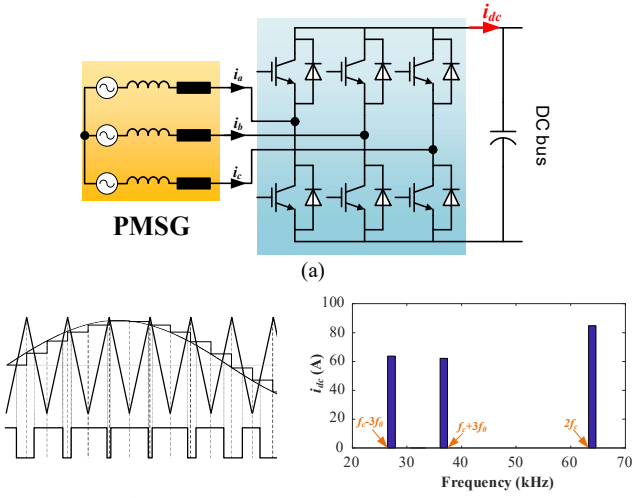

Fig. 2. Two-level three-phase converter. a) PMSG and 2-level converter, b) asymmetric regular sampling PWM, c) spectrum of i_{dc}.

The converter and PWM method have been widely used in AC-DC conversion. Fig. 2c shows the spectrum of i_{dc} which is the current flowing into the capacitor from the converter side. It shows significant components of $f_c \pm 3f_0$ and $2f_c$. Here, f_c is the switching frequency, f_0 is the fundamental frequency from PMSG. For dual-channel generation system, generators driven by HP and LP shafts always work under different speeds and thus generate electrical power with different fundamental frequencies. This means harmonics of $f_c \pm 3f_0$ are difficult to

suppress because of fixed f_c together with variable f_0. However, harmonic on $2f_c$ has a better potential of suppression due to no influence from f_0. Using double Fourier solution illustrated in [21], analysis of this spectrum will be presented in the following section.

A. Mathematical analysis on DC-bus 2nd carrier harmonic

Assuming the current on the AC side is ideally sinusoidal for a two-level converter, AC side currents can be written as

$$i_{ac}^{[k]}(t) = I_{ac}\cos\left(2\pi f_0 t + \beta + \frac{2k\pi}{3}\right) \quad (1)$$

where I_{ac} is the amplitude of the fundamental component of AC current, f_0 is the fundamental frequency, β is the angle between phase current and its AC side voltage, k=0, 1 and 2 represent phase A, B and C respectively.

Assuming the positive current on DC bus i_{dc} is from the converter to the dc-link capacitor as shown in Fig. 2. Asymmetrical regular sampling PWM is analysed here because of better voltage output performance compared to symmetric sampling. The switching function of it for each phase leg can be expressed by

$$sf^{[k]}(t) = K_{0,1}\cos\left(2\pi f_0 t + \beta + \alpha + \frac{2k\pi}{3}\right) + \sum_{m=1}^{\infty}\sum_{n=-\infty}^{\infty} K_{m,n}\cos\left[m\left(2\pi f_c t + \theta_c^{[k]}\right) + n\left(2\pi f_0 t + \beta + \alpha + \frac{2k\pi}{3}\right)\right] \quad (2)$$

where f_c is the switching frequency, $\theta_c^{[k]}$ is phase angle of the triangular carrier signal for each leg, α is the phase angle between AC fundamental current and AC-side converter voltage (i.e. power factor angle), $K_{m,n}$ is the harmonic amplitude using the Bessel function of the first kind. Based on double Fourier analysis[21], $K_{m,n}$ can be expressed by

$$K_{m,n} = \frac{1}{q_{m,n}} J_n(q_{m,n}M)\sin\left[(m+n)\frac{\pi}{2}\right] \quad (3)$$

$$q_{m,n} = \left(m + n\frac{f_0}{f_c}\right)\frac{\pi}{2} \quad (4)$$

In (3) and (4), $J_n()$ is Bessel function of the first kind. m and n are orders of switching harmonic and its side bands respectively. For instance, when m=1 and n=3, $K_{m,n}$ means the magnitude of harmonic with a frequency of f_c+3f_0. Using (1) – (4), the DC-bus harmonic currents generated from one phase leg can be derived as

$$\begin{aligned} i_{dc}^{[k]}(t) &= i_{ac}^{[k]}(t)sf^{[k]}(t) \\ &= \frac{I_{ac}}{2}\left\{K_{0,1}\left[\cos\left(4\pi f_0 t + 2\beta + \alpha + \frac{4k\pi}{3}\right) + cos\alpha\right]\right. \\ &+ \sum_{m=1}^{\infty}\sum_{n=-\infty}^{\infty} K_{m,n}\left\{\cos\left[2\pi(mf_c + (n+1)f_0)t + \sigma_{m,n}^{[k]}\right]\right. \\ &\left.\left. + \cos\left[2\pi(mf_c + (n-1)f_0)t + \varphi_{m,n}^{[k]}\right]\right\}\right\} \end{aligned} \quad (5)$$

Where $\sigma_{m,n}^{[k]}$ and $\varphi_{m,n}^{[k]}$ are phase angles of each component, which are

$$\sigma_{m,n}^{[k]} = m\theta_c^{[k]} + (n+1)\left(\beta + \frac{2k\pi}{3}\right) + n\alpha \quad (6)$$

$$\varphi_{m,n}^{[k]} = m\theta_c^{[k]} + (n-1)\left(\beta + \frac{2k\pi}{3}\right) + n\alpha \quad (7)$$

With (5), the current harmonics on DC-bus should be expressed as a sum of three legs' harmonics as

$$\begin{aligned} i_{dc,i,j}(t) &= \frac{I_{ac}}{2}K_{i,j-1}\sum_{k=0}^{2}\cos\left[2\pi(if_c + jf_0)t + \sigma_{i,j-1}^{[k]}\right] \\ &+ \frac{I_{ac}}{2}K_{i,j+1}\sum_{k=0}^{2}\cos\left[2\pi(if_c + jf_0)t + \varphi_{i,j+1}^{[k]}\right] \end{aligned} \quad (8)$$

Where i and j mean switching and band side orders of DC-bus current harmonics. For instance, i and j equal 1 and 3 when harmonic on fc+3f_0 is analyzed. i and j are different from m and n, because m and n are orders for switching function.

Considering no phase shift on carrier signals among three legs, i.e. $\theta_c^{[1]} = \theta_c^{[2]} = \theta_c^{[3]}$, the phase angle of each component in (8) can be given as

$$\sigma_{i,j-1}^{[k]} = i\theta_c^{[k]} + j\left(\beta + \frac{2k\pi}{3}\right) + (j-1)\alpha \quad (9)$$

$$\varphi_{i,j+1}^{[k]} = i\theta_c^{[k]} + j\left(\beta + \frac{2k\pi}{3}\right) + (j+1)\alpha \quad (10)$$

From (8) – (10), it can be concluded that current components $i_{dc,i,j}$ (t) are zeros apart from cases with j=0, ±3, ±6, etc. This is due to fact that the three-phase currents are of 2π/3 phase shift and the characteristic of sinusoidal functions that

$$cos\theta + cos\left(\theta + \frac{2k\pi}{3}\right) + cos\left(\theta + \frac{4k\pi}{3}\right) = 0 \quad (11)$$

Expression in (8) can be divided into two components. The magnitudes of both components can be derived as

$$\frac{I_{ac}K_{i,j-1}}{2} = \frac{I_{ac}}{2q_{i,j-1}}J_{j-1}(q_{i,j-1}M)\sin\left[(i+j-1)\frac{\pi}{2}\right] \quad (12)$$

$$\frac{I_{ac}K_{i,j+1}}{2} = \frac{I_{ac}}{2q_{i,j+1}}J_{j+1}(q_{i,j+1}M)\sin\left[(i+j+1)\frac{\pi}{2}\right] \quad (13)$$

It can be seen from (12) and (13) that, when i+j are odd numbers (2k+1, k = 0, 1, 2, 3, ….), the magnitudes of these harmonics are zeros. Thus, only cases when i+j are even numbers need to be studied.

In summary, the dc current harmonics only appear when

$$j = 0, \pm 3, \pm 6 \ldots \quad (14)$$

$$i + j = \text{even number} \quad (15)$$

Hence, only components with frequency f_c±3f_0 (i=1, j=±3) and 2f_c (i=2, j=0) harmonics will appear at the dc-link side. The cases when i >2 and j>6 are generally not considered since the magnitudes are small and have little influence on capacitor ripples. This is in line with the diagram shown in Fig. 2c.

In this paper, suppression of harmonics with a frequency of 2f_c will be focused. From (8), substitute i=2 and j=0, the 2nd order carrier harmonic current generated from three-phase converter (with three legs) can be derived as

$$\begin{aligned} i_{dc,2,0}(t) = \frac{3I_{ac}}{2}\{&K_{2,-1}cos[4\pi f_c t + 2\theta_c - \alpha] \\ &+ K_{2,1}cos[4\pi f_c t + 2\theta_c + \alpha]\} \end{aligned} \quad (16)$$

B. Simplified model on 2nd carrier harmonic

According to (16), two components with the same frequency

but different magnitudes and phase angles can be derived as

$$\frac{3I_{ac}}{2}K_{2,-1}cos(4\pi f_c t + 2\theta_c - \alpha) \text{ and}$$
$$\frac{3I_{ac}}{2}K_{2,1}cos(4\pi f_c t + 2\theta_c + \alpha) \quad (17)$$

The coefficient $K_{2,1}$ and $K_{2,-1}$ are written as

$$K_{2,1} = -\frac{2}{(2+\frac{f_0}{f_c})\pi}J_1(\frac{\pi}{2}(2+\frac{f_0}{f_c})M) \quad (18)$$

$$K_{2,-1} = -\frac{2}{\left(2-\frac{f_0}{f_c}\right)\pi}J_1(\frac{\pi}{2}(2-\frac{f_0}{f_c})M) \quad (19)$$

Assuming that $f_c >> f_0$ (in normal cases, f_c is at least 20 times of f_0), the term f_0/f_c can be neglected as it is approximately equal to 0. Substituting f_0/f_c =0 to (18) and (19) gives

$$K_{2,1} \approx K_{2,-1} \approx -\frac{1}{\pi}J_1(\pi M) \quad (20)$$

Substituting (20) to (16) and using characteristic of sinusoidal functions

$$i_{dc,2,0}(t) \approx -\frac{3I_{ac}cos\alpha}{\pi}J_1(\pi M)\cos(4\pi f_c t + 2\theta_c) \quad (21)$$

From (21), it can be seen that power factor angle α will have no impact on the phase angle of $I_{dc,2,0}(t)$. This is very important and useful conclusion, since the power factor angle α is always determined by operating conditions of generators, including rotating speed, output power and dc-link voltage etc. Decoupling the power factor and the harmonic phase angle will significantly simplify the development of harmonic cancellation strategies.

For a given output converter power P, the AC-side terminal real power of the two-level converter can be formulated as

$$P = 3\frac{I_{ac}}{\sqrt{2}}\frac{V_{ac}}{\sqrt{2}}\cos\alpha = \frac{3I_{ac}MV_{dc}}{4}\cos\alpha \quad (22)$$

where V_{ac} is the magnitude of converter phase voltage, M is the modulation index of the converter. It can be derived from (22) that

$$I_{ac}cos\alpha = \frac{4P}{3MV_{dc}} \quad (23)$$

combining (23) and (21) gives

$$i_{dc,2,0}(t) \approx \frac{4PJ_1(\pi M)}{\pi MV_{dc}}\cos(4\pi f_c t + 2\theta_c)$$
$$= \frac{4I_{dc}J_1(\pi M)}{\pi M}\cos(2\times 2\pi f_c t + 2\theta_c) \quad (24)$$

where I_{dc} is the DC component of the current i_{dc} on DC-bus. From (24), it is important to note that the magnitude of the 2nd carrier harmonic current is only influenced by DC-link current (I_{dc}) and modulation index (M) in the simplified model. Meanwhile, the phase angle of this component is determined by the angle of the carrier signal (θ_c) only. This means that the phase angle of second carrier harmonic on DC-bus current can be controlled by carrier signal θ_c within the AC/DC converter.

C. Comparison between the simplified and original model

The comparison between original (16) and simplified (24) model of DC-bus second carrier harmonics is given in Fig 3 using the generation system developed in [22]. The generator parameters are given in Table I. The system is essentially composed of a permanent magnet generator and a two-level converter. Fig 3a compares the magnitude of $I_{dc,2,0}(t)$ between the simplified and original models and Fig. 3b compares the angle phase difference between results from these two models. The modulation index is set as 0.95 during the calculation. This is reflecting the fact that the generator is always operated at high-speed and a flux-weakening is applied with high modulation index for the converter operations.

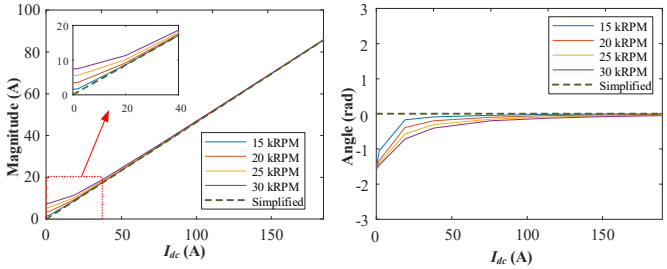

(a) (b)

Fig. 3. Comparison of second carrier harmonic component ($I_{dc,2,0}(t)$) from original and simplified models with increased generator power and speed. (a) Magnitude; (b) Phase angle.

In Fig 3a and b, a relatively bigger error can be noticed with an increase of the PMSM generator speed. This is due to the fact that the fundamental frequency is increased with fast rotating PMSMs and the assumption of f_0/f_c=0 in (19) will produce increased errors. However, accuracy of the simplified model is still acceptable, especially when the power is higher than 10kW (I_{dc} >37A with a 270Vdc).

TABLE I
SIMULATION PARAMETERS

Category	Parameters	Values
PMSG parameters	Number of poles	6
	Resistance	1.058 mΩ
	Machine inductance	99 μH
	Flux linkage of permanent magnet	0.03644 Vs/rad
	DC link voltage reference	270 V
	Switching frequency	16 kHz
	Maximum modulation index	0.95
	Rated power	45kW
Simulation parameters	DC link capacitance	200 μF
	Load resistance	1.35 Ω
	Rotor speed	From 15 kRPM to 30 kRPM

In addition, when the power is below 10kW, it is obvious that magnitude is not significant. It is understood that the harmonic magnitude under this condition will not be significant due to the smaller current. With the power increase, the power factor α will move towards to zero. This is due to the fact that more active power has been generated by the electrical generator while the reactive power (used for de-fluxing) kept almost the same. From (16), two components on the right side of the equation are symmetric, this means improvement of the accuracy of the simplification.

From Fig.3a, magnitude is always less than 20A when the power is less than 10kW (I_{dc}<37A, power factor less than 0.21) compared to almost 80A when the power is 45kW (I_{dc}=166.6A, power factor at 0.83). In practice, we are more interested in high-power operation and this is the operation region where

power quality issues should be more carefully addressed.

III. PROPOSED METHOD

Using the developed simplified model, a second carrier harmonic cancellation method will be proposed and discussed in this section. In Fig. 4a, the dual-channel generation system is shown in more details. As can be seen, the dual-channel generation system is controlled by a centralized controller. The controller detailed in Fig 4b is used to regulate the DC-bus voltage and apply different power sharing strategy based on system optimization. Both PMSG1 and PMSG2 are operated under flux weakening control because of wide rotor speed range[22].

A. Method for 1:1 power sharing ratio

When generators supply equal power to the system, and two converters operate under the same modulation index, approximately same magnitude of the second harmonic can be achieved using

$$\frac{4I_{dc1}J_1(\pi M)}{\pi M} = \frac{4I_{dc2}J_1(\pi M)}{\pi M} \tag{25}$$

where I_{dc1} and I_{dc2} are DC components of current i_{dc1} and i_{dc2}. Considering two sinusoidal currents flowing into one node and these two currents are of the same amplitude and frequency, it can be concluded that these harmonic currents will sum up to zero if they are of 180-degree phase shift. From (25), we can conclude that, to make the 2nd harmonics of dc currents from two power converters with the same magnitude, the average dc current and the modulation index should be the same for the two power converters, i.e. I_{dc1}=I_{dc2} and M_1=M_2. In order to cancel the 2nd harmonics, the phase angle difference $(2\theta_c^{[1]} - 2\theta_c^{[2]})$ should be 180 degrees. This suggests that the phase difference between the two carrier signals $(\theta_c^{[1]} - \theta_c^{[2]})$ should be 90 degrees. Here, superscripts [1] and [2] are the indices of generators.

Based on this fact, a phase shifter with a fixed phase shift angle (90 degrees) is applied within the control system as shown in Fig 4b. This proposed solution with a fixed shift angle is much simpler compared to those discussed by other researchers[18][19].

B. Method for non-average power sharing ratio

For optimizing fuel consumption and surge margin of the engine, it is very common that the two generation systems are not with the same power[23][24]. In these cases, applying 90-degree phase shift may not give expected results with entirely eliminated the 2nd carrier harmonics. This is because the magnitudes of 2nd carrier components are different. To overcome this problem, an additional 2nd carrier harmonic magnitude adaptor should be applied as shown in Fig.4.

Define K as power sharing ratio between two sources which is

$$K = \frac{i_{ref1}}{i_{ref2}} \tag{26}$$

Hence, the current references, i_{ref1} and i_{ref2}, to the two converters can be expressed as

$$\begin{cases} i_{ref1} = i_{ref}\dfrac{K}{K+1} \\ i_{ref2} = i_{ref}\dfrac{1}{K+1} \end{cases} \tag{27}$$

The same magnitudes of 2nd carrier harmonics should be achieved with

$$\frac{4i_{ref1}J_1(\pi M_1)}{\pi M_1} = \frac{4i_{ref2}J_1(\pi M_2)}{\pi M_2} \tag{28}$$

From (28), modulation index (M_1 and M_2) of each converter can be actively controlled to achieve same 2nd carrier harmonic magnitude between two sources. From (24) or (28), it can be noted that smaller modulation index will result in higher harmonic magnitude. As shown in Fig. 1, assuming that PMSG1 is driven by HP shaft and PMSG2 driven by the LP shaft. Extracting higher power from LP shaft than HP shaft will help increase surge margin for engine[23][24]. Hence, K is always less than 1. With K<1, PMSG1 will produce less power than

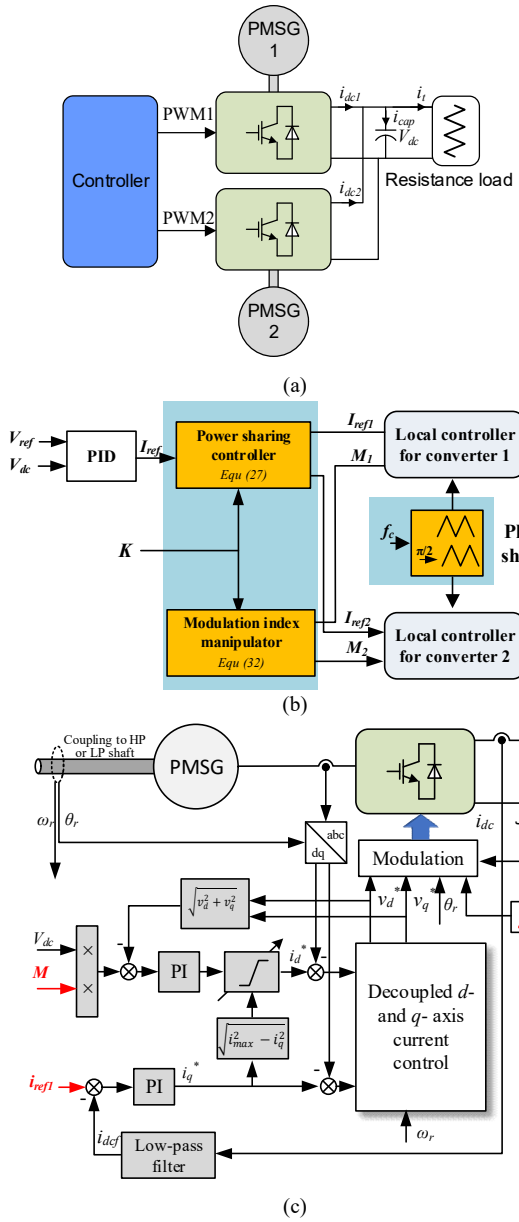

Fig. 4. Control diagram of the proposed method. (a) System diagram, b) Zoom out of controller in a), c) Local controller.

PMSG2.

As PMSGs operate under flux-weakening control region, the modulation index can be adjusted in controller. With the same modulation index between two PMSGs, the 2nd order harmonic from PMSG1 system is lower than that from PMSG 2 because of its lower DC-bus current (as PMSG1 produce less active power). Reducing modulation index for PMSG 1 system, however, its 2nd order harmonic will be increased according to (24). Thus reducing the modulation index in PMSG1 can compensate the impact of reduced power such that the 2nd carrier harmonic reach the same magnitude of that from PSMG2. Using (24) and assuming $M_2 = M_{high}$, the relationship between two magnitudes can be expressed as

$$\frac{4i_{ref1}J_1(\pi M_1)}{\pi M_1} = \frac{4i_{ref2}J_1(\pi M_{high})}{\pi M_{high}} \tag{29}$$

from (29) and (26), we have

$$\frac{J_1(\pi M_1)}{M_1} = \frac{J_1(\pi M_{high})}{KM_{high}} \tag{30}$$

Define a function

$$f(M) = \frac{J_1(\pi M)}{M} \tag{31}$$

The desired modulation index for the PSMG1 system M_1 can be derived as

$$M_1 = f^{-1}\left(\frac{J_1(\pi M_{high})}{KM_{high}}\right) \tag{32}$$

This inverse function is hard to calculate in real-time controller due to complicated Bessel function. Hence, a look-up table is applied in practical cases. Fig 5 shows the relationship between M and K when M_{high}=0.9 and 0.95 respectively. For a specific power sharing K, the modulation index M of PSGM1 associated converter can be derived using look-up table in Fig.5.

Local controller is shown in Fig 4c. Control parameters set from Fig 4b (M, i_{ref}, carrier signal) are highlighted in red. For flux-weakening control under optimized modulation index, the outer voltage control loop provides a negative reference for d-axis current. Meanwhile, an adjustable saturation block is applied. It is to prevent AC side current over the limit i_{max}.

Using adapted modulation index and 90-degree phase shift on carrier signal, 2nd carrier harmonics on DC-bus capacitor can be suppressed in different power sharing ratio cases.

C. First band harmonic

In previous sections, the modulation index of one converter within LP power generation channel is actively controlled, which helps further reduction of the second harmonic. However, the 1st band harmonics (f_c±3f_0) also play important role in current spectrum. Hence, these two components are investigated in this section.

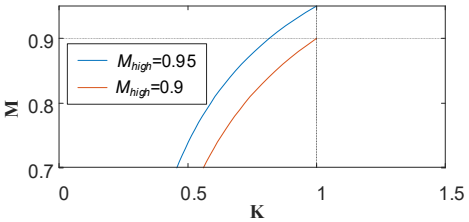

Fig. 5. M-K look-up figure model.

Firstly, harmonic on f_c+3f_0 is analyzed. Substitute i=1 and j=3 into (8) gives

$$i_{dc,1,3}(t) = \frac{3I_{ac}}{2}K_{1,2}cos\left[2\pi(f_c+3f_0)t+\sigma_{1,2}\right] + \frac{3I_{ac}}{2}K_{1,4}cos\left[2\pi(f_c+3f_0)t+\varphi_{1,4}\right] \tag{33}$$

For the coefficient $K_{1,2}$ and $K_{1,4}$, we have

$$K_{1,2} = -\frac{2}{(1+2\frac{f_0}{f_c})\pi}J_2\left(\frac{\pi}{2}(1+2\frac{f_0}{f_c})M\right) \tag{34}$$

$$K_{1,4} = \frac{2}{\left(1+4\frac{f_0}{f_c}\right)\pi}J_4\left(\frac{\pi}{2}(1+4\frac{f_0}{f_c})M\right) \tag{35}$$

Again, if we assume that $f_c >> f_0$, the term f_0/f_c can be neglected. The equation (32) can be approximated as

$$i_{dc,1,3}(t) \approx -\frac{3I_{ac}}{\pi}J_2\left(\frac{\pi}{2}M\right)\cos\left[2\pi(f_c+3f_0)t+\sigma_{1,2}\right] + \frac{3I_{ac}}{\pi}J_4\left(\frac{\pi}{2}M\right)cos\left[2\pi(f_c+3f_0)t+\varphi_{1,4}\right] \tag{36}$$

Repeat the same process, the harmonic on f_c-3f_0 can be approximately expressed as

$$i_{dc,1,-3}(t) \approx \frac{3I_{ac}}{\pi}J_4\left(\frac{\pi}{2}M\right)\cos\left[2\pi(f_c-3f_0)t+\sigma_{1,-4}\right] - \frac{3I_{ac}}{\pi}J_2\left(\frac{\pi}{2}M\right)cos\left[2\pi(f_c-3f_0)t+\varphi_{1,-2}\right] \tag{37}$$

These formulas (36) and (37) are difficult to be further simplified. The results are determined by generator parameters and operation points. However, the first-band harmonic components of DC-link current I_{dc} and the modulation index M can be identified using numeral analysis and are shown in Fig.6. Here, PMSM parameters are shown in Table I and the fundamental frequency is assumed f_0=1,200Hz. Systems with other fundamental frequencies can be analysed in a similar way. The change of the fundamental frequency will not have impacts to the conclusions and will not be detailed in this paper. Analysis on other PMSM parameters is another future study which will not be illustrated here.

As illustrated in Fig 5, modulation of PMSG 1 is less than M_{high} with K<1 (i.e. more electrical power is extracted from the LP shaft). From Fig 6, magnitudes of f_c±3f_0 harmonics decrease if the modulation index decreases. Recalling that reducing modulation index of PMSG1 are used to make its 2nd carrier harmonic component equivalent to that of PMSG2 system. It can be concluded that adaptively reducing the modulation index of PMSG1 can potentially suppress both first sideband (f_c±3f_0)

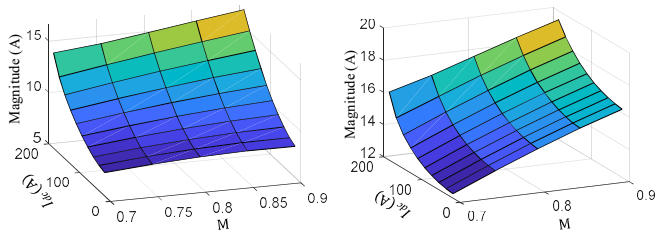

Fig. 6. Magnitudes of first band harmonics related to the modulation and dc-link current. a) f_c-3f_0, b) f_c+3f_0.

and second switching harmonic $2f_c$ harmonics. This will be further demonstrated using simulation and experimental test below.

IV. Simulation and Experiment Results

A. Simulation results

The simulation was implemented on MATLAB/Simulink and PLECS to evaluate the performance of proposed harmonic model and cancellation method. Some basic control parameters for a multi-source power system are shown in Table I.

Fig 7a shows how the proposed method works. With power sharing ratio decrease from 1:1 to 0.8:1, M_1 is adjusted based on (32). Moreover, currents before capacitor are controlled where filtered currents change to 89A and 110A respectively under 0.8:1.

Fig 7b and c show the spectrums of currents on converter DC-link and capacitor when power sharing ratio is 1:1 and 0.8:1 respectively. Results under two operations are shown on both spectrums, which are a) constant modulation index (0.95) with no phase shift, b) constant modulation index with 90 degrees phase shift. Another operation of c) optimized modulation index with 90 degrees phase shift (here, M_1=0.895, M_2=0.95) is only shown on Fig 3c, because modulation index needs no variation when the power sharing ratio is 1:1. It can be seen that constant modulation index with 90 degrees phase shift has significantly suppressed the 2nd carrier harmonic on the DC-bus capacitor. Moreover, with variable modulation index, the component is further suppressed when the power sharing ratio is 0.8:1, which validate the harmonic cancellation under non-average power sharing ratio. Meanwhile,1st band harmonic in Fig 3c is also validated that reducing the modulation index will not increase first band harmonic in most cases.

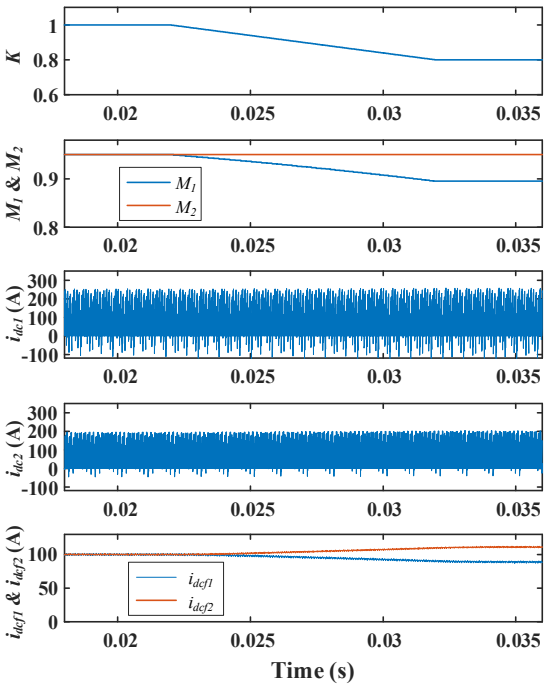

(a)

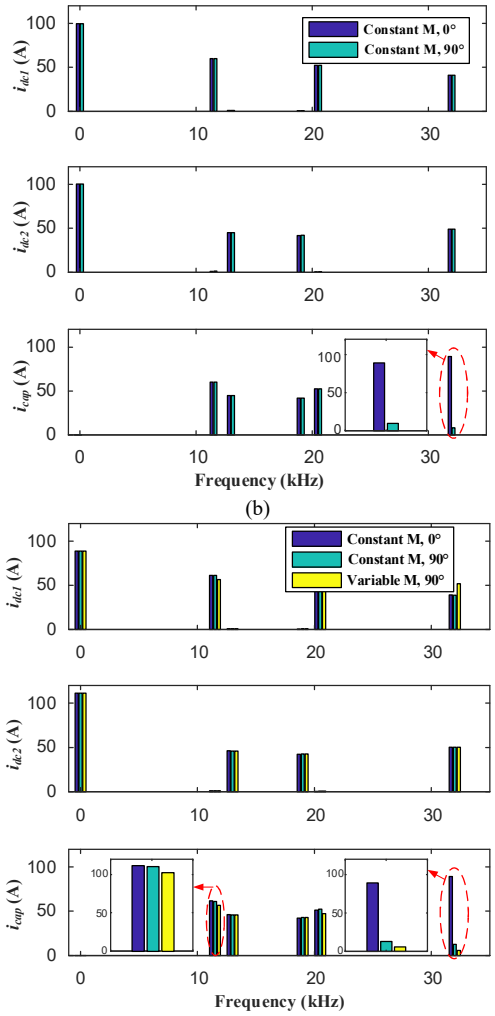

(b)

(c)

Fig. 7. Current spectrums when power sharing ratio changes from 1:1 to 0.8:1. a) Simulation result of proposed cancellation method. b) Current spectrum when K=1:1. c) Current spectrum when K=0.8:1.

B. Experiment results

In the experiment, PMSGs are replaced by a grid and programmable AC source. Schematic diagram and the test rig are shown in Fig. 8a and Fig. 8b respectively. A 3-phase isolated transformer and a variac are located between inductors and AC source in order to prevent ring current between two converters. The system is controlled using DSK6713 TI DSP augmented with FPGA boards. Unlike using rotor position sensor in PMSGs, phase-locked loop (PLL) is implemented in

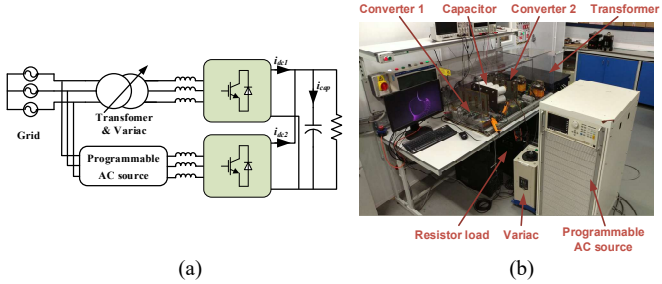

(a) (b)

Fig. 8. Experiment setup. (a) Schematic drawing. (b) Physical drawing.

TABLE II
EXPERIMENT PARAMETERS

Parameters	Values
DC link capacitance	4.4 mF
Line inductance	1 mH
DC bus voltage	270V
Load resistance	40 Ω
Frequencies of AC side	50 Hz and 60 Hz
Line-to-line voltages of AC side	250 V
Switching frequency	4 kHz
Maximum modulation index	0.95

the controller to achieve phase angle of fundamental voltage.

The parameters of the experiment are shown in Table II. Output frequencies of the grid and programmable AC source are 50Hz and 60Hz respectively to represent different fundamental frequencies among PMSGs. The switching frequency is 4kHz which is much higher than fundamental frequencies. The line-to-line voltages of AC side are 250Vrms, whose peak value is far more than DC-link reference value.

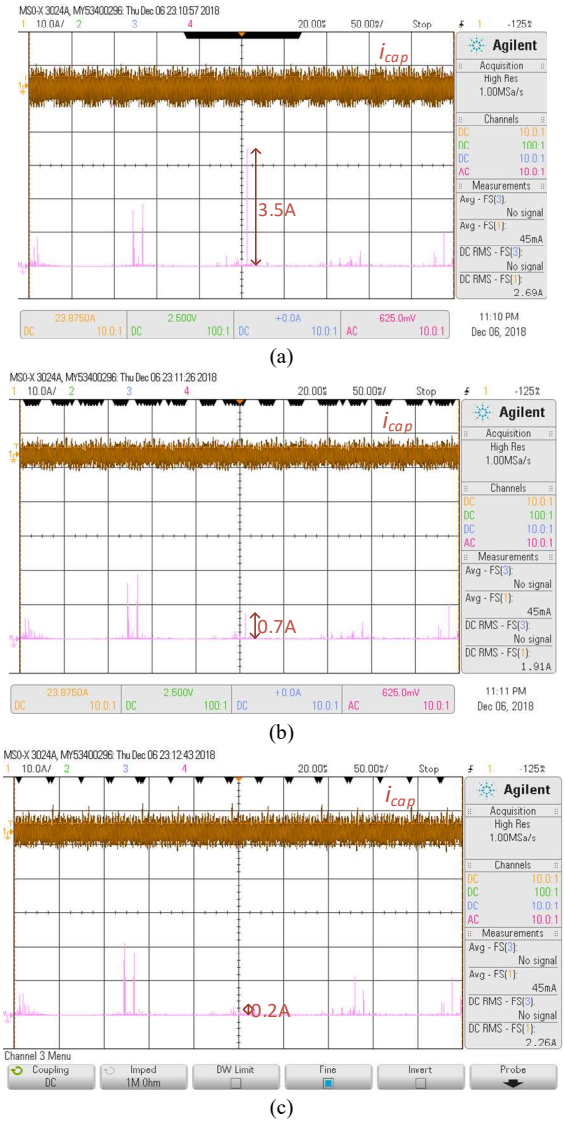

Fig. 9. Capacitor currents and their spectrums when power sharing ratio is 0.8:1. (a) No phase shift and no optimized modulation index. (b) With 90-degree phase shift without optimized modulation index. (c) 90-degree phase shift together with optimized modulation index.

Hence, converters must operate under flux-weakening control, where the modulation index can be manipulated. The maximum modulation index is set as 0.95. Power sharing ratio is 0.8:1 between converters as same as that in simulation.

Fig 9a-c show the capacitor current (i_{cap}) under a) constant M (0.95) with no phase shift, b) constant M with 90 degrees phase shift, and c) variable M with 90 degrees phase shift. Magnitudes of the 2nd carrier harmonic were tagged in figures. The 2nd carrier harmonic is suppressed from 3.5A to 0.7A when only applying a 90-degree phase shift on the carrier signal. A 80% suppression ratio was achieved. Then, this magnitude was further suppressed to 0.2A (a further 14% reduction) when optimized modulation index applied.

Compare Fig 9b and c, there is a little increase on the first band harmonic. The reason is experiment is not based on PMSM with parameters in Table I because of limitation of test rig. Meanwhile, the study has not considered about the power loss on converter, which will also cause increase on first band harmonics. These issues can be further studied in future.

V. CONCLUSIONS

In this paper, a simplified mathematical model on 2nd carrier current harmonic was investigated. The results show the magnitude of the component was only determined by the value of DC current and modulation index, while the phase angle of it is caused by the carrier phase angle.

Based on a simplified model, a 2nd harmonic cancellation method was proposed. By actively controlling modulation index together with 90-degree phase shift on the carrier signal, a cancellation can be realized in a 2-source power system. The method can work under any machine speed and need no communication of harmonic phase angle among sources.

The simplified model and cancellation method are basic research of harmonic cancellation. It gives potential approach of harmonic cancellation in not only dual-generator system, but also other multi-converter systems such as microgrid or back-to-back converter.

Finally, simulation and experiment were implemented to verify the validity of the proposed 2nd carrier harmonic model and cancellation method.

REFERENCES

[1] Sarlioglu, Bulent, and Casey T. Morris. "More electric aircraft: Review, challenges, and opportunities for commercial transport aircraft." *IEEE transactions on Transportation Electrification* 1, no. 1 (2015): 54-64..

[2] F. Gao, S. Bozhko, G. Asher, P. Wheeler, and C. Patel, "An Improved Voltage Compensation Approach in a Droop-Controlled DC Power System for the More Electric Aircraft," *IEEE Transactions on Power Electronics*, vol. 31, no. 10, pp. 7369–7383, 2016.

[3] P. Wheeler and S. Bozhko, "The more electric aircraft: Technology and challenges," *IEEE Electrification Magazine*, vol. 2, no. 4, pp. 6–12, 2014.

[4] F. Gao, S. Bozhko, A. Costabeber, G. M. Asher, and P. W. Wheeler, "Control design and voltage stability analysis of a droop-controlled electrical power system for more electric aircraft," *IEEE Trans. Ind. Electron.*, vol. 64, no. 12, pp. 9271–9281, Dec. 2017.

[5] Y. Jia and K. Rajashekara, "An Induction Generator-Based AC/DC Hybrid Electric Power Generation System for More Electric Aircraft," *IEEE Trans. Indus. Appl*., vol. 53, no. 3, pp. 2485-2494, June 2017.

[6] X. Lang, T Yang, H. B. Enalou, S. Bozhko, and P. Wheeler. "An Enhanced Power Generation Centre for More Electric Aircraft Applications." In *2018 IEEE International Conference on Electrical Systems for Aircraft, Railway, Ship Propulsion and Road Vehicles & International Transportation Electrification Conference (ESARS-ITEC)*, pp. 1-6. IEEE, 2018.

[7] H. B. Enalou, S. Bozhko, M. Rashed, and et. al., "A Preliminary Study into Turbofan Performance with LP-HP Power Exchange," *in GPPS Global Power & Propulsion Society*, Montreal, 2018.

[8] B.-G. Gu and K. Nam, "A DC-link capacitor minimization method through direct capacitor current control," *IEEE Trans. Ind. Appl*., vol. 42, no. 2, pp. 573–581, Mar./Apr. 2006.

[9] R. Maheshwari, S. Munk-Nielsen, and K. Lu, "An active damping technique for small DC-Link capacitor based drive system," *IEEE Trans. Ind. Informat*., vol. 9, no. 2, pp. 848–858, May 2013.

[10] B. P. McGrath and D. G. Holmes, "A general analytical method for calculating inverter DC-link current harmonics," *IEEE Transactions on Industry Applications*, vol. 45, no. 5, pp. 1851–1859, 2009.

[11] F. D. Kieferndorf, M. Förster, and T. A. Lipo, "Reduction of DC-bus capacitor ripple current with PAM/PWM converter," *IEEE Transactions on Industry Applications*, vol. 40, no. 2, pp. 607–614, 2004.

[12] T. D. Nguyen, N. Patin, and G. Friedrich, "Extended double carrier PWM strategy dedicated to RMS current reduction in DC link capacitors of three-phase inverters," *IEEE Transactions on Power Electronics*, vol. 29, no. 1, pp. 396–406, 2014.

[13] L. Xi, and F. Z. Peng. "Theoretical analysis of DC link capacitor current ripple reduction in the HEV DC-DC converter and inverter system using a carrier modulation method." In *2012 IEEE Energy Conversion Congress and Exposition (ECCE)*, pp. 2833-2839. IEEE, 2012.

[14] Z. Pan and R. A. Bkayrat, "Modular motor/converter system topology with redundancy for high-speed, high-power motor applications," *IEEE Transactions on Power Electronics*, vol. 25, no. 2, pp. 408–416, 2010.

[15] T. Suzuki, Y. Hayashi, H. Kabune, and N. Ito, Pulsewidth Modulation Control Algorithm for a Six-Phase PMSM: Reducing the Current in the Inverter Capacitor and Current Sensing with Resistors. *IEEE Transactions on Industrial Electronics*, *66*(6), 4240-4249, 2019.

[16] G. Gohil, R. Maheshwari, L. Bede, T. Kerekes, R. Teodorescu, M. Liserre, and F. Blaabjerg, "Modified discontinuous PWM for size reduction of the circulating current filter in parallel interleaved converters," *IEEE Transactions on Power Electronics*, vol. 30, no. 7, pp. 3457–3470, 2015.

[17] X. Xing, C. Zhang, A. Chen, H. Geng, and C. Qin, "Deadbeat Control Strategy for Circulating Current Suppression in Multiparalleled Three-Level Inverters," *IEEE Transactions on Industrial Electronics,* vol. 65, no. 8, pp. 6239–6249, 2018.

[18] L. Shen, S. Bozhko, G. Asher, C. Patel, and P. Wheeler, "Active DC Link Capacitor Harmonic Current Reduction in Two-Level Back-to-Back Converter," *IEEE Transactions on Power Electronics*, vol. 31, no. 10, pp. 6947–6954, 2016.

[19] L. Shen, S. Bozhko, C. I. Hill, and P. Wheeler, "DC-Link Capacitor Second Carrier Band Switching Harmonic Current Reduction in Two-Level Back-to-Back Converters," *IEEE Transactions on Power Electronics*, vol. 33, no. 4, pp. 3567–3574, 2018.

[20] C. Wang, T. Yang, S. Bozhko, and P. Kulsangcharoen. "An enhanced second carrier harmonic cancellation method for multi-source DC electric power systems." In *IECON 2019-45th Annual Conference of the IEEE Industrial Electronics Society*, vol. 1, pp. 2610-2615. IEEE, 2019.

[21] T. Lipo and D. G. Holmes, Pulse Width Modulation for Power Converters. 2003.

[22] S. Bozhko, T. Yang, J.M. Le Peuvedic, P. Arumugam, M. Degano, A. La Rocca, Z. Xu et al. "Development of Aircraft Electric Starter–Generator System Based on Active Rectification Technology." *IEEE transactions on transportation electrification* 4, no. 4 (2018): 985-996.

[23] H. B. Enalou, S. Bozhko, M. Rashed, and P. Kulsangcharoen. "A Preliminary Study into Turbofan Performance with LP-HP Power Exchange." In *GPPS Global Power & Propulsion Society*. 2018.

[24] R. Todd., F. Bryan, A. J. Forsyth, C. Gan, and J. Bossard. "Effects of electrical power off-take on finite inertia mechanical systems." In *2011 IEEE Energy Conversion Congress and Exposition*, pp. 1476-1482. IEEE, 2011.

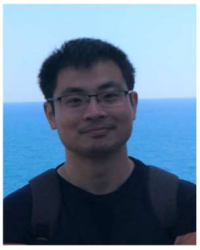

Cheng Wang was born in Jiangsu, China. He received the B.Eng. and M.Sc. degrees in electrical engineering from Nanjing University of Aeronautics and Astronautics, Nanjing, China, in 2013 and 2016, respectively. Since 2017, he has been working toward the Ph.D. degree with the Power Electronics, Machines and Control Group, University of Nottingham, Nottingham, U.K.

His research interests include control and power quality improvement in area of electric DC power systems.

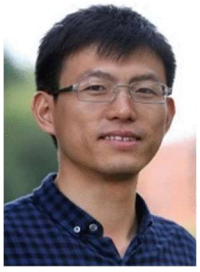

Tao Yang (M'16–SM'20) received the Ph.D. degree in electrical engineering from the University of Nottingham, Nottingham, U.K., in 2013.

Since then, he has been a Researcher and an Associate Professor with the Power Electronics, Machines and Control Group, University of Nottingham. His research interests include aircraft electrical power systems and high-speed motor drives for aerospace applications.

Ponggorn Kulsangcharoen (M'19) received the BEng., MSc., and PhD. degrees in electrical and electronic engineering from the University of Nottingham, Nottingham, U.K., in 2007, 2008, and 2013, respectively.

During 2013 and 2018, he was a researcher with the Power Electronics, Machines and Controls Research Group (PEMC), University of Nottingham and was involved in the design and development of grid-interface power converters for energy storage applications funded by E.ON and aircraft engine emulator system funded by Clean Sky2. He is currently with Collins Aerospace working on machine drives and power supplies for aerospace applications.

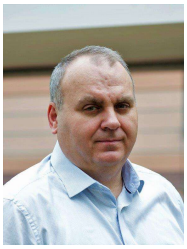

Serhiy Bozhko (M'96–SM'18) was born in City, Country. He received the M. and SM. and F. degrees in electrical engineering from University of City, Country in 1999, 2004 and 2009 respectively.

Since 2000, he has been with the Power Electronics, Machines and Controls Research Group of the University of Nottingham, United Kingdom, where currently he is Professor of Aircraft Electric Power Systems and Director of the Institute for Aerospace Technology. He is leading several EU- and industry funded projects in the area of aircraft electric power systems, including power generation, distribution and conversion, power quality, control and stability issues, power management and optimization, as well as advanced modelling and simulations methods.